JOURNAL OF BACTERIOLOGY, June 1992, p. 3487–3493
0021-9193/92/113487-07$02.00/0

Vol. 174, No. 11

Permeability and Charge-Dependent Adsorption Properties of the S-Layer Lattice from *Bacillus coagulans* E38-66

MARGIT SÁRA,* DIETMAR PUM, AND UWE B. SLEYTR

Zentrum für Ultrastrukturforschung und Ludwig Boltzmann-Institut für Molekulare Nanotechnologie, Universität für Bodenkultur, A-1180 Vienna, Austria

Received 26 December 1991/Accepted 18 March 1992

We investigated the permeability properties of the oblique S-layer lattice from *Bacillus coagulans* E38-66 after depositing cell wall fragments on a microfiltration membrane, cross-linking the S-layer protein with glutaraldehyde, and degrading the peptidoglycan with lysozyme. Comparative permeability studies on such multilayered S-layer membranes and suspended S-layer vesicles from thermophilic members of the family *Bacillaceae* with use of the space technique (M. Sára and U. B. Sleytr, J. Bacteriol. 169:4092–4098, 1987) revealed identical molecular exclusion limits (M. Sára and U. B. Sleytr, J. Membr. Sci. 33:27–49, 1987). Examination of the S-layer lattice from *B. coagulans* E38-66 with the S-layer membrane technique revealed unhindered passage for molecules up to the size of myoglobin (M_r 17,000). The molecular dimensions of this protein (2.8 by 3.2 by 4.5 nm) correspond approximately to the size of the ovoid-shaped pore previously shown by high-resolution electron microscopy of negatively stained S-layer self-assembly products (D. Pum, M. Sára, and U. B. Sleytr, J. Bacteriol. 171:5296–5303, 1989). Chemical modification of the S-layer protein and comparative labeling, adsorption, and permeability studies clearly demonstrated that (i) in the native state, free amino and carboxyl groups are present on the outer S-layer face and in the interior of the pores and (ii) electrostatic interactions between these groups prevent unspecific adsorption of the S-layer in vivo.

Many procaryotic organisms possess crystalline surface layers (S-layers) as their outermost cell envelope component (for compilations, see references 14, 22, and 24). S-layer lattices, which are composed of identical protein or glycoprotein subunits, show oblique, square, or hexagonal symmetry (2–3a, 8–10, 14, 21–23). In analogy to other bacterial cell surface structures, S-layers have most likely evolved as a consequence of interactions between the organism and its natural, frequently quite competitive habitat (3a, 14, 22, 23, 25). Among other functions, S-layers have been suggested to act as protective molecular sieves, particularly representing barriers to hostile macromolecules such as lytic enzymes (3, 10, 22, 23). Nevertheless, the S-layers from thermophilic members of the family *Bacillaceae* studied so far cannot be considered as effective protective coats since they possess pores with sizes of 4 to 5 nm, which still allow the passage of proteins with molecular weights of up to 45,000 (18, 19), including muramidases and proteases.

The ultrastructure and the self-assembly process of the S-layer of the highly thermophilic *Bacillus coagulans* E38-66 have been described in detail in a previous report (15). The S-layer lattice shows oblique symmetry with lattice constants of a = 9.4 nm, b = 7.4 nm, and $\gamma = 80°$. The apparent molecular weight of the S-layer protein on sodium dodecyl sulfate gels was found to be 100,000. In the three-dimensional model of the mass distribution of the S-layer protein which was derived from negatively stained S-layer self-assembly products, two different types of pores could be observed. The dimension of the ovoid-shaped pore was in the range of 2.8 by 3.2 nm, whereas the size of the S-shaped pore was about 4.5 by 2.0 nm (15).

In this study, we have investigated the molecular-sieving properties of the S-layer from *B. coagulans* E38-66 and compared the data with the size of the pores derived from the previously described three-dimensional model (15). For obtaining information on the location of charged groups on the S-layer lattice and on their interactions with macromolecules, chemical modification of the S-layer protein and comparative adsorption and permeability experiments were performed.

MATERIALS AND METHODS

Bacterial strain and growth conditions. *B. coagulans* E38-66 was kindly provided by F. Hollaus (Österreichisches Zuckerforschungsinstitut, Vienna, Austria). Cells were grown in continuous culture at 63°C under the conditions given previously (15).

Cell wall preparation and S-layer self-assembly conditions. Cell wall preparation and extraction of the S-layer subunits with guanidine hydrochloride (5 M in 50 mM Tris-HCl buffer, pH 7.2) was performed as described previously (15). Guanidine hydrochloride extracts were dialyzed against distilled water for 18 h at 20°C.

Treatment of cell wall fragments with glutaraldehyde and lysozyme. Cross-linking of the S-layer protein in cell wall fragments with glutaraldehyde (0.5% in 0.1 M sodium cacodylate buffer, pH 7.2) and digestion of the peptidoglycan-containing layer with lysozyme were done as described previously (18). Samples were then prepared for ultrathin sectioning, which was performed according to the procedure given in reference 17.

Labeling of the native and chemically modified outer S-layer face with PCF. Glutaraldehyde treatment of whole cells and chemical modification of free carboxyl groups after activation with 1-ethyl-3,3′-dimethyl (aminopropyl) carbodiimide (EDC) and reaction with glycine methyl ester (GME) were done as described previously (17) according to the procedure of Carraway and Koshland (5). Native, glutaraldehyde-treated whole cells and cells modified with EDC and GME were labeled with polycationized ferritin (PCF) as described

* Corresponding author.

TABLE 1. Rejection coefficients of S-layer membranes prepared from S-layer material of *B. coagulans* E38-66

Protein	M_r (10^3)	Molecular size (nm)	Rejection coefficient (percentile rejection)[a]
Cyt *c*	12	2.5 by 2.5 by 3.7	0
Myoglobin	17	2.5 by 3.5 by 4.5	0
Carbonic anhydrase	30	4.1 by 4.1 by 4.7	90
Ovalbumin	43		100
BSA	67	4.0 by 4.0 by 14.0	100
Ferritin	440	12	100

[a] Calculated according to the equation worked out for batch ultrafiltration procedures (4).

TABLE 2. Relative flux losses of SMs after filtration of the different protein solutions

Protein	M_r (10^3)	pI	RF loss (1 − RF)[a]		
			A	B	C
Cyt *c*	12	10.8	0.74	0.68	0.10
Myoglobin	17	6.8	0.73	0.63	0.08
Carbonic anhydrase	30	5.3	0.67	0.60	0.04
Ovalbumin	43	4.6	0.00	0.00	0.08
BSA	67	4.7	0.04	0.05	0.06
Ferritin	440	4.3	0.00	0.00	0.10
PCF	440	11	0.10	0.10	0.10

[a] Relative water flux (RF) is calculated as RF = J_A/J_0, where J_A is water flux after protein filtration and J_0 is initial water flux. Data represent relative flux losses before (column A) and after (column B) degradation of the peptidoglycan-containing layer with lysozyme and relative flux losses of SMs in which the carboxyl groups were converted into neutral groups by amidation (column C).

previously (17). PCF binding was evaluated by electron microscopy (EM) using freeze-etched preparations.

Permeability studies using SMs produced from cell wall fragments. The permeability properties of the S-layer of *B. coagulans* E38-66 were determined after depositing native cell wall fragments on a microporous support, cross-linking the S-layer protein with glutaraldehyde, and degrading the peptidoglycan-containing layer with lysozyme. For this purpose, 0.13 g of cell wall fragments (wet pellet, obtained after centrifugation at 20,000 × *g* for 20 min) was suspended in 50 ml of 10 mM $CaCl_2$. Five milliliters of this suspension was used for coating nylon microfiltration membranes with a diameter of 62 mm (type PALL Ultipor N_{66}; nominal pore size, 0.1 μm), which was done in a closed ultrafiltration cell (Amicon type 8050) at a pressure of 2 × 10^5 Pa. Subsequently, the deposited cell wall material was stabilized by cross-linking the S-layer protein with glutaraldehyde (0.5% in 0.1 M sodium cacodylate buffer, pH 7.2) for 20 min at 20°C. The detailed procedure for producing S-layer membranes (SMs) and testing the integrity of the active filtration layer consisting of the S-layer material is described elsewhere (19). For determining the rejection characteristics of SMs, disks with a diameter of 25 mm were punched out and inserted into 10-ml ultrafiltration cells (Amicon type 8010). The permeability studies were carried out as ultrafiltration experiments as follows. The test proteins with increasing molecular weights (Table 1) were dissolved at 0.4 to 0.8 mg/ml of distilled water; 4 ml of the feed solution was concentrated by a factor of 4 at a pressure of 2 × 10^5 Pa and a stirring speed of 500 rpm. The protein concentrations in the feed solution, in the permeate, and in the retentate were determined at 280 nm in a Beckman model DU-65 spectrophotometer. The rejection coefficients (given as percentile rejection; Table 1) were calculated according to the equation worked out for batch ultrafiltration procedures (4): $R = (\log c_r - \log c_0)/\log n$, where R is the rejection coefficient, c_r is the concentration in the retentate, c_0 is the concentration in the feed solution, and n is the concentration factor.

For degrading the peptidoglycan, SMs were treated with lysozyme (50 μg/ml of 50 mM Tris-HCl buffer, pH 7.2) for 1 h at 37°C, washed for at least 6 h with Tris-HCl buffer, and tested as described before.

Adsorption properties of SMs. Flux losses of ultrafiltration membranes after filtration of solutions of macromolecules (e.g., proteins) generally indicate adsorption of these molecules in the pores (12, 16). For determining the influence of the peptidoglycan-containing layer on protein adsorption, SMs were used before and after degradation of the rigid cell wall layer with lysozyme. For all SMs, the water flux was determined with distilled particle-free water (MilliQ quality) before and after filtration of 3 ml of the different protein solutions through the 25-mm disks. After careful removal of the retentate, the membrane surface was rapidly rinsed with 10 ml of distilled water for removal of loosely adsorbed protein (12). Then, 10 ml of distilled water was added to the ultrafiltration cell and stirred for 5 min at 20°C. This procedure was repeated two times before the water flux was measured again. Membrane adsorption was expressed in terms of the relative flux loss (Table 2). The relative flux loss is 0 if no adsorption has occurred and 1 if the pores are completely blocked by adsorbed material.

Chemical modification of carboxyl groups on SMs. Carboxyl groups of the S-layer protein were activated with EDC and converted into neutral groups by reaction with GME. The reaction conditions were those given in reference 19.

Binding of PCF and cyt *c* to S-layer self-assembly products adsorbed to EM grids. Adsorption of S-layer self-assembly products to EM grids was done as described previously for the negative-staining procedure (15). After the grids were washed with distilled water, the adsorbed S-layer self-assembly products were either immediately fixed with glutaraldehyde (0.5% in 0.1 M sodium cacodylate buffer, pH 7.2) for 20 min or first floated on drops of a cytochrome *c* (cyt *c*; Sigma C-7752) or PCF (Sigma F-7879) solution (each at 10 mg/ml of distilled water) for 20 min. Samples which were first fixed with glutaraldehyde were transferred onto a drop of Tris-HCl buffer (50 mM, pH 7.2), incubated for 10 min to stop the reaction, extensively washed with distilled water for 10 min, and subsequently floated on drops of a cyt *c* solution. After being washed with distilled water, the cyt *c*-labeled samples were postfixed with glutaraldehyde. Native, PCF-labeled, or cyt *c*-labeled preparations were also washed with distilled water for 2 min and then fixed with glutaraldehyde. Negative staining was done with uranyl acetate (1% in distilled water) for 2 min. EM was performed with a Philips 301 transmission electron microscope (TEM) and a Philips CM12 TEM/scanning stem, using the low-dose facility.

Binding of cyt *c* to suspended S-layer monolayers. Two milliliters of a suspension from S-layer monolayers containing 2 mg of S-layer protein per ml of distilled water was centrifuged at 20,000 × *g* for 10 min and resuspended in 2 ml of a cyt *c* solution (2 mg/ml of distilled water; Sigma C-7752). After 20 min of incubation at 20°C, the suspension was centrifuged and the pellet was washed once in 2 ml of distilled water. Both supernatants were collected, and the concentration of cyt *c* was determined in a Beckman model

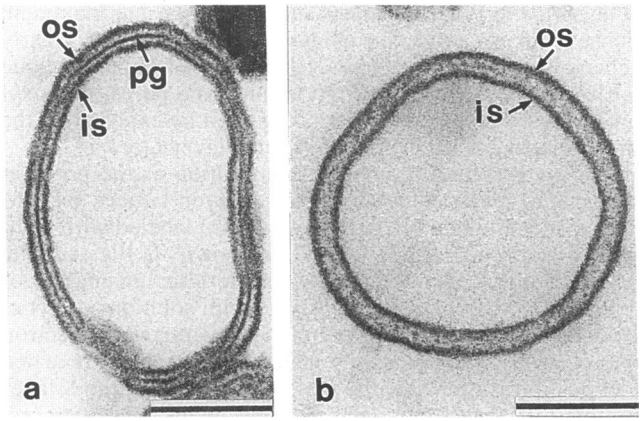

FIG. 1. Electron micrographs of ultrathin sections from cell wall fragments of *B. coagulans* E38-66 after cross-linking of the S-layer protein with glutaraldehyde (a) and degradation of the peptidoglycan with lysozyme (b). os, outer S-layer; is, inner S-layer; pg, peptidoglycan. Bars, 200 nm.

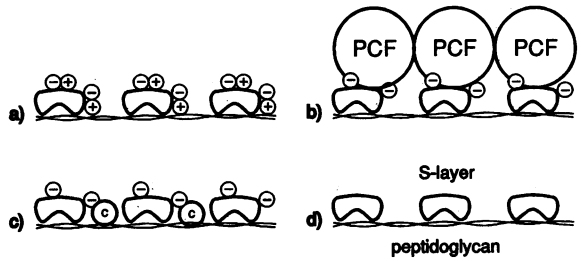

FIG. 2. Schematic drawing illustrating the adsorption of the net positively charged proteins PCF and cyt *c* (c) to the S-layer lattice from *B. coagulans* E38-66. The outer face of the S-layer lattice was accessible in whole cells and in SMs produced from cell wall fragments. The outer face of the S-layer lattice was not capable of binding PCF in the native state (a) but was densely labeled with PCF after cross-linking of the S-layer protein with glutaraldehyde (b), which caused the loss of the positively charged amino groups. After treatment of the S-layer protein with glutaraldehyde, cyt *c* could adsorb to free carboxyl groups in the interior of the pores (c). No adsorption of either marker molecule was observed after conversion of free carboxyl groups in glutaraldehyde-treated S-layer lattices into neutral groups by amidation (d).

DU-65 spectrophotometer at 280 nm. The amount of cyt *c* adsorbed per S-layer subunit was calculated as described previously (15).

Image processing. Micrographs were examined with an optical diffractometer and selected for subsequent computer image processing when several high-resolution spots were found beyond a 1/2.0 nm^{-1} threshold. Micrographs were scanned with a raster spacing corresponding to approximately 0.7 nm on the original object. Digitized images (1,024 by 1,024 pixels) were processed on a 386 personal computer equipped with a high-resolution visual graphics assembly display adaptor and monitor (1,024 by 768 pixels). Both cross-correlation averaging (20) and Fourier domain processing (1) were used for processing of image data; amplitudes and phases of the diffraction maxima were interpolated with the use of a peak-profile fitting procedure (11). Symmetry-related pairs were complex averaged and submitted to the back transformation. Finally, reconstructed projection maps of the protein mass distribution were displayed as half-tone images or output was displayed as isodensity lines on a pen plotter. Software for all processing steps was written by D. Pum.

RESULTS

Treatment of cell wall fragments with lysozyme. Ultrathin sections of glutaraldehyde-treated cell wall fragments revealed a three-layered cell envelope profile (Fig. 1a) which consisted of the outer S-layer, the peptidoglycan-containing layer, and an inner S-layer whose subunits are known to assemble on the inner face of the rigid cell wall layer during extraction of the plasma membrane (21). Lysozyme treatment of cell wall fragments in which the S-layer protein was cross-linked with glutaraldehyde led to the degradation of the peptidoglycan-containing layer (Fig. 1b). The distance between the outer and the inner S-layers was in the range of 5 to 10 nm, which corresponded to the thickness of the degraded rigid cell wall layer.

Labeling of the native and chemically modified outer face of the S-layer lattice with PCF. Freeze-etched preparations of whole cells which were incubated with PCF revealed that the outer face of the native S-layer lattice was not capable of binding this strongly positively charged topographical marker (not shown). After treatment of whole cells with glutaraldehyde, which induces loss of the positive charge on the amino groups, the S-layer surface was densely labeled with PCF (Fig. 2). After conversion of free carboxyl groups into neutral groups by amidation, no PCF molecules were detected on glutaraldehyde-treated whole cells (Fig. 2). Since PCF is too large to enter the pores, the results clearly demonstrated the presence of free amino and carboxyl groups on the protein domains on the outer S-layer face. Amino and carboxyl groups are obviously involved in direct electrostatic interactions in the native state of the crystal lattice.

Permeability studies on S-layers arranged as a coherent layer on a microfiltration membrane. Permeability studies were carried out as ultrafiltration experiments. For producing SMs, cell wall fragments were deposited on a microfiltration membrane such that a coherent layer was formed before the S-layer protein was cross-linked with glutaraldehyde. Ultrathin sections of the composite SMs showed that a closed multilayer structure consisting of up to three superimposed layers of cell wall fragments was formed on the surface of the microfiltration membrane (not shown). The integrity of SMs was checked by filtration of a ferritin solution (M_r of 440,000; molecular size of 12 nm; pI 4.3). Since ferritin is larger than one morphological unit in the S-layer lattice, it must be completely rejected by an intact coherent filtration layer. Thus, only SMs for which no ferritin could be detected in the permeate were used for further permeability studies. As derived from the rejection coefficients (Table 1), SMs allowed free passage for cyt *c* and myoglobin (molecular weights of 12,000 and 17,000, respectively) but were completely impermeable for the larger test proteins ovalbumin and bovine serum albumin (BSA) (molecular weights of 43,000 and 67,000, respectively). Carbonic anhydrase (molecular weight of 30,000) was rejected to 90%. SMs revealed the same rejection properties before and after degradation of the peptidoglycan-containing layer with lysozyme. This finding demonstrated that in cell wall fragments prepared according to the described procedure, the pores in the heteroporous peptidoglycan meshwork must be larger than those in the S-layer lattice.

Adsorption properties of S-layers in SMs. SMs showed no

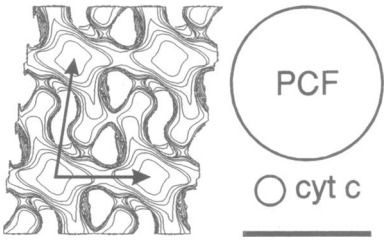

FIG. 3. Image reconstruction of the top view of the outer face of the oblique S-layer lattice from *B. coagulans* E38-66 and the relative sizes of PCF and cyt *c* used for the labeling experiments. a = 9.4 nm, b = 7.4 nm, γ = 80°. PCF has a molecular size of 12 nm. Cyt *c*, having a molecular size of 2.5 by 2.5 by 3.7 nm, was small enough to pass through the pores. Arrows indicate base vectors. Bar, 10 nm.

or negligible flux losses after filtration of solutions of ferritin, BSA, or ovalbumin (Table 2). Because of their isoelectric points, these test proteins possessed a net negative charge in distilled water (pH 5.3), which obviously prevented adsorption to the net negatively charged S-layer lattice obtained by cross-linking the S-layer protein with glutaraldehyde. After filtration of solutions of cyt *c* (pI 10.8) or myoglobin (pI 6.8), which revealed a positive net charge in distilled water and which were small enough to pass through the pores, SMs showed flux losses of up to 70%. This finding indicated adsorption of the protein molecules in the interior of the pores. By contrast, flux losses after filtration of solutions containing the strongly positively charged but larger PCF (pI 11; molecular size of 12 nm) were in the range of only 10%. Although freeze-etching of glutaraldehyde-treated whole cells demonstrated the presence of a monolayer of PCF on the outer face of the S-layer lattice (Fig. 2), there was obviously enough space between the spherical PCF molecules to allow the passage of water molecules through the adsorbed monolayer to the lattice pores. The molecular sizes of PCF and cyt *c* in relation to that of the S-layer subunits are shown in Fig. 3. After filtration of solutions of carbonic anhydrase, which was rejected to at least 90%, SMs revealed flux losses of approximately 70%, corresponding to the data obtained for myoglobin and cyt *c*. Since carbonic anhydrase is only slightly larger than the ovoid-shaped pore, the high flux losses can be explained by pore plugging due to the adsorption of the protein molecules noted above, but not in the interior of the pores. To investigate the importance of negatively charged groups for adsorption of macromolecules, carboxyl groups of the S-layer protein were activated with EDC and modified with GME. Carboxy-amidated SMs showed flux losses of only up to 10% after filtration of solutions of either cyt *c*, myoglobin, or carbonic anhydrase solutions (Table 2). These results confirmed that free carboxyl groups arranged in the pore areas were responsible for protein adsorption of glutaraldehyde-treated nonmodified S-layer lattices.

Flux losses of lysozyme-treated SMs were comparable to those of untreated membranes, indicating that adsorption to the S-layer lattice and not to the peptidoglycan-containing layer was the limiting factor.

Binding of PCF and cyt *c* to S-layer self-assembly products adsorbed to EM grids. In previous studies, it was demonstrated that monolayers of S-layer self-assembly products (Fig. 4a) adsorbed with their charge-neutral outer face to glow-discharged EM grids (15). In this orientation, the net negatively charged inner S-layer face was exposed and could be labeled with PCF (Fig. 4b). As shown by negative staining (Fig. 4b), the PCF molecules did not reveal the maximum dense packing order on S-layer monolayers but clearly reflected the orientation of the base vectors from the oblique lattice. Since PCF is too large to enter the pores, carboxyl groups responsible for PCF binding must be exposed on the protein domains on the native inner S-layer face.

For investigating the charge distribution at the pores in native and glutaraldehyde-treated S-layer lattices by EM methods, self-assembly monolayers were labeled with cyt *c* after adsorption to EM grids. As shown in Fig. 4c, the oblique lattice was still clearly visible after incubation of adsorbed native S-layer monolayers with solutions of cyt *c*. Both Fourier filtering and correlation averaging of electron micrographs from negatively stained preparations revealed identical projections for the mass distribution of the S-layer protein for labeled and unlabeled specimens. Although resolution (1.5 to 1.7 nm) and sampling interval (0.7 nm) were too small to allow the localization of cyt *c*, no additional molecules could be visualized in the reconstructions (not shown). On the other hand, comparative adsorption studies with suspended S-layer monolayers revealed that 250 μg of cyt *c* was bound per mg of S-layer protein, which corresponds to two cyt *c* molecules per S-layer subunit. Since the presence of free carboxyl groups on the protein domains on the inner S-layer face was known from PCF labeling, it was concluded that the cyt *c* molecules had bound to the S-layer protein domains, but they were obviously too small to be distinguished from the bulky mass of the S-layer protein.

Self-assembly monolayers which were cross-linked with glutaraldehyde before labeling with cyt *c* revealed only a grainy appearance in negatively stained preparations (Fig. 4d). Since the crystalline S-layer structure could be detected only by low-order-intensity maxima in diffractograms, it was concluded that the cyt *c* molecules had randomly bound to the inner face of the S-layer lattice, covering both the protein domains and the pore areas. The random binding of the positively charged cyt *c* molecules was also demonstrated by a deterioration of the resolution in the diffractograms due to strong variations of the staining patterns in the individual unit cells (not shown). Binding of cyt *c* in the pores of the glutaraldehyde-treated S-layer lattice demonstrated that the net negative charge had been generated upon blocking the free amino groups with glutaraldehyde. In the native state, charges from free amino and carboxyl groups are obviously neutralized by direct electrostatic interactions (Fig. 5).

DISCUSSION

Our experiments represent the first attempt to compare the permeability properties of an S-layer lattice with the pore size and the morphology characterized by high-resolution electron microscopy of negatively stained S-layer self-assembly products. The permeability properties of the S-layer from *B. coagulans* E38-66 were determined by applying ultrafiltration techniques on SMs. Previous studies on two strains of *Bacillus stearothermophilus* possessing square and hexagonal S-layer lattices have shown that the rejection characteristics derived from SMs were identical to the permeability properties obtained for isolated S-layer vesicles with the space technique (18, 19). Independent of the applied method, both the square and hexagonal S-layer lattices allowed free passage for myoglobin (M_r 17,000) and carbonic anhydrase (M_r 30,000) but rejected ovalbumin (M_r 43,000) to at least 90%. These results confirmed that the rejection characteristics from SMs were exclusively determined by the molecular-sieving properties of the individual S-layer

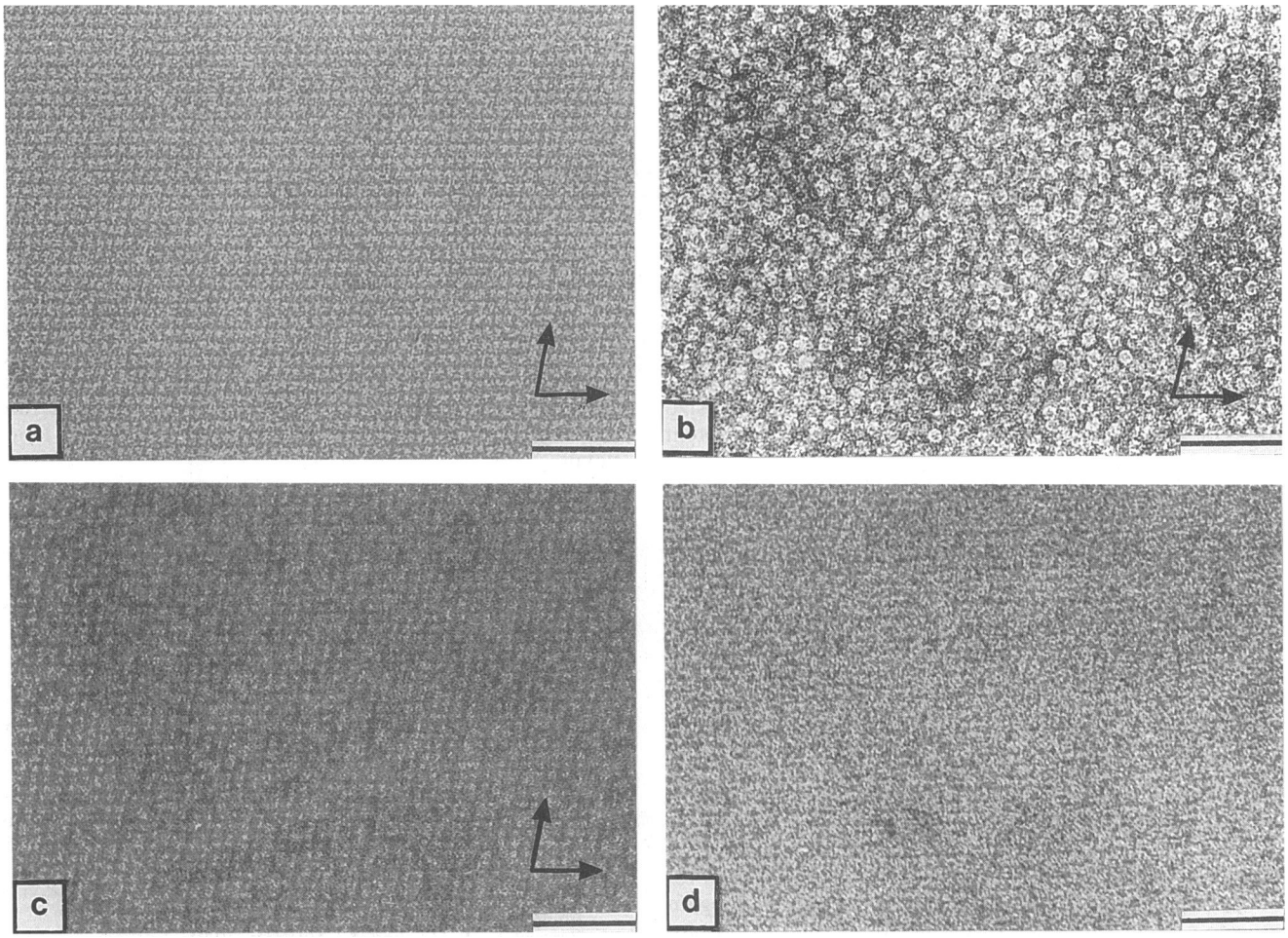

FIG. 4. Electron micrographs of negatively stained S-layer self-assembly products from *B. coagulans* E38-66. The native monolayers adsorbed with the outer face to the EM grids. (a) Native monolayer revealing an oblique lattice; (b) native monolayer labeled with PCF; (c and d) monolayer labeled with cyt *c* before (c) and after (d) cross-linking the S-layer protein with glutaraldehyde. Arrows indicate base vectors. Bars, 100 nm.

monolayers, although the active filtration layer consisted of up to three superimposed layers in the form of either cell wall fragments or isolated S-layer sheets.

By applying the SM technique in this study, it was shown that the S-layer lattice from *B. coagulans* E38-66 allowed free passage for myoglobin but rejected carbonic anhydrase to 90%. If myoglobin penetrates in lengthwise orientation, pores with a size of at least 2.5 by 3.5 nm are required. This is in the range of the size of the ovoid-shaped pore observed in the three-dimensional model of the S-layer lattice.

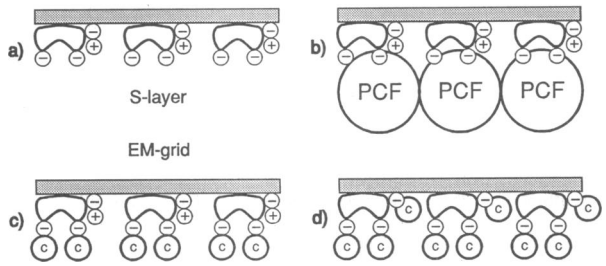

FIG. 5. Schematic drawing illustrating the adsorption of the net positively charged proteins PCF and cyt *c* (c) to the S-layer lattice from *B. coagulans* E38-66. The inner face of the S-layer lattice revealing a net negative surface charge was exposed on self-assembly monolayers which had adsorbed to EM grids (a) and could therefore be labeled with PCF (b). Binding of cyt *c* in the interior of the pores did not occur in the native state (c) but was possible after cross-linking of the S-layer protein with glutaraldehyde (d).

Considering the S-layer of *B. coagulans* E38-66 as a crystalline protein network exhibiting two morphologically well-defined types of pores, the fact that up to 10% of carbonic anhydrase was detected in the permeate can be explained in different ways. One reason for the incomplete rejection of carbonic anhydrase might be seen in the poor long-range order of the oblique S-layer lattice of *B. coagulans* E38-66 (15). Freeze-etching of whole cells revealed that the S-layer lattice consisted of differently oriented crystallites which completely covered the cell surface (15). Because of the presence of numerous crystal boundaries, it cannot be excluded that pores larger than the original lattice pores are generated at these imperfections, which could be responsible for the leakage of carbonic anhydrase.

A further reason for the incomplete rejection of carbonic anhydrase can be seen in the possibility of dynamic structural changes and fluctuations occurring in the S-layer sub-

units. Studies on soluble proteins have shown that among the high number of molecules present in a solution, a large number of conformational substates may exist (6). Transitions occurring among the substates are equilibrium fluctuations, whereas transitions from one conformational state to another require changes of the environmental conditions (6). Considering the possibility of such equilibrium fluctuations in the native state of the S-layer lattice, it can be assumed that not all of the large number of constituent subunits will have the same conformational substate at the moment when the cross-linking reaction with glutaraldehyde occurs. Consequently, the observed deviations in the molecular-sieving properties of an ideal isoporous S-layer lattice may be explained simply by trapping domains of the subunits at diverse substates or states of their conformation. In the case of carbonic anhydrase, only a slight increase in the pore size would be sufficient to allow its passage through the protein network.

Neither the presence of pores larger than the lattice pores in the areas of the grain boundaries of the crystalline array nor variations in size of only a small number of pores induced by a conformational mobility of the constituent subunits can be detected by computer image reconstruction procedures based on unit cell averaging such as Fourier domain techniques or cross-correlation averaging. Finally, to some degree, differences between the pore size determined by EM methods and that derived from permeability studies can be explained by the uncertainty in defining the boundaries between the heavy-metal stain and the protein in the reconstructions (for a detailed discussion, see reference 7). Usually this threshold is chosen as the boundary between protein and stain where the gradient in contrast is steepest while at the same time the protein network must stay contiguous. This approach is particularly successful in reconstructions which show a high contrast in a narrow region between protein and stain. When the contrast variations are low over the entire image, however, dramatic changes in the resulting structure may be created by only slight variations in the interactively determined threshold levels. In addition, the quality of the reconstruction itself depends on factors such as artifacts introduced during specimen preparation and radiation damage-induced alterations.

Our data on the adsorption studies further suggest that charges from free amino and carboxyl groups exposed on the outer face of the native S-layer lattice and in the interior of the pores are neutralized by direct electrostatic interactions. Thus, in accordance with all other S-layers of thermophilic and mesophilic members of the family *Bacillaceae* so far studied, the S-layer lattice of *B. coagulans* E38-66 masks the net negative surface of the peptidoglycan (15, 17). Since the S-layer lattice represents the outermost cell envelope component, all initial interactions of the living cell with molecules or particles present in the natural habitat of the organism will be determined by the physicochemical properties of the crystalline network. The permeability and adsorption studies clearly showed that the S-layer prevents nonspecific adsorption of macromolecules, which can be seen as an essential requirement to prevent pore plugging and to maintain an unhindered transport of low-molecular-weight substances (e.g., nutrients and metabolites) and the secretion of exoproteins. On the other hand, it cannot be excluded that ions and small charged molecules such as amino acids, vitamins, or nucleotides can bind to charged groups on the S-layer lattice at domains not accessible for macromolecules. In previous studies, it was shown that filtration of lysine solutions through SMs did not cause flux losses (16a), although it is likely that lysine adsorbs to free carboxyl groups present in glutaraldehyde-treated S-layer lattices. Thus, it seems that molecules with a size in the range of amino acids are too small to cause detectable pore plugging. To conclude, the native S-layer lattice from *B. coagulans* E38-66 can be considered as a rather charge neutral molecular sieve allowing an unhindered passage for molecules with molecular weights of up to 17,000. As observed for other thermophilic members of the family *Bacillaceae*, S-layers with pores of this size cannot be considered effective protective barriers. On the other hand, the pores could determine the speed of release of the organism's own exoproteins (e.g., exoenzymes) or even prevent their liberation. A restricted diffusion may also guarantee a complete folding of the polypeptide chains into their three-dimensional, more protease-resistant structure (7a). We are currently investigating this aspect in more detail.

ACKNOWLEDGMENTS

Part of this work was supported by the Bundesministerium für Wissenschaft und Forschung and the Fonds zur Förderung der wissenschaftlichen Forschung in Österreich, Projekt S50/02 and S57/05.

REFERENCES

1. **Amos, L., R. Henderson, and P. N. T. Unwin.** 1982. Three-dimensional structure determination by electron microscopy of two-dimensional crystals. Prog. Biophys. Mol. Biol. **39:**183–231.
2. **Baumeister, W., and H. Engelhardt.** 1987. Three-dimensional structure of bacterial surface layers, p. 109–154. *In* J. R. Harris and R. W. Horne (ed.), Electron microscopy of proteins, vol. 6. Membraneous structure. Academic Press, London.
3. **Beveridge, T. J.** 1981. Ultrastructure, chemistry and function of the bacterial cell wall. Int. Rev. Cytol. **72:**229–317.

3a. **Beveridge, T. J., and L. Graham.** 1991. Surface layers of bacteria. Microbiol. Rev. **55:**684–705.

4. **Blatt, W.** 1976. Principles and practice of ultrafiltration, p. 81–120. *In* P. Meares (ed.), Membrane separation processes. Elsevier, Amsterdam.
5. **Carraway, K. L., and D. E. Koshland, Jr.** 1972. Carbodiimide modification of proteins. Methods Enzymol. **25:**616–623.
6. **Creighton, T. E.** 1989. Protein function. IRL Press, Oxford.
7. **Engelhardt, H.** 1988. Correlation averaging and 3-D reconstruction of 2-D crystalline membranes and macromolecules. Methods Microbiol. **20:**357–415.

7a. **Glenn, A. R.** 1976. Production of extracellular proteins by bacteria. Annu. Rev. Microbiol. **30:**41–62.

8. **Hovmöller, S., A. Sjögren, and D. N. Wang.** 1988. The structure of crystalline bacterial cell surface layers. Prog. Biophys. Mol. Biol. **51:**131–163.9.
9. **Kandler, O., and H. König.** 1985. Cell envelopes of archaebacteria, p. 413–457. *In* C. R. Woese and R. S. Wolfe (ed.), The bacteria, vol. 8. Archaebacteria. Academic Press, Inc., New York.
10. **Koval, S. F.** 1988. Paracrystalline protein surface arrays on bacteria. Can. J. Microbiol. **34:**407–414.
11. **Kübler, O.** 1980. Unified processing of periodic and nonperiodic specimens. J. Microsc. Spectrosc. Electronmicrosc. **5:**561–575.
12. **Matthiasson, E.** 1983. The role of macromolecule adsorption in fouling of ultrafiltration membranes. J. Membr. Sci. **16:**23–26.
13. **Messner, P., D. Pum, and U. B. Sleytr.** 1987. Characterization of the ultrastructure and the self-assembly of the surface layer (S layer) of *Bacillus stearothermophilus* NRS2004/3a. J. Ultrastruct. Mol. Struct. Res. **97:**73–88.
14. **Messner, P., and U. B. Sleytr.** 1992. Crystalline bacterial cell surface layers. Adv. Microb. Physiol. **33:**213–275.
15. **Pum, D., M. Sára, and U. B. Sleytr.** 1989. Structure, surface charge and self-assembly of the S-layer lattice from *Bacillus*

coagulans E38-66. J. Bacteriol. **171**:5296–5303.
16. **Reihanian, H., C. R. Roberts, and A. S. Micheals.** 1983. Mechanisms of polarization and fouling of ultrafiltration membranes by proteins. J. Membr. Sci. **16**:237–258.
16a. **Sára, M.** Unpublished data.
17. **Sára, M., and U. B. Sleytr.** 1987. Charge distribution on the S layer of *Bacillus stearothermophilus* NRS1536/3c and importance of charge groups for morphogenesis and function. J. Bacteriol. **169**:2804–2809.
18. **Sára, M., and U. B. Sleytr.** 1987. Molecular sieving through S layers of *Bacillus stearothermophilus* strains. J. Bacteriol. **169**: 4092–4098.
19. **Sára, M., and U. B. Sleytr.** 1987. Production and characteristics of ultrafiltration membranes with uniform pores from two-dimensional arrays of proteins. J. Membr. Sci. **33**:27–49.
20. **Saxton, W. O., and W. Baumeister.** 1984. Three-dimensional reconstruction of imperfect two-dimensional crystals. Ultramicroscopy **13**:57–70.
21. **Sleytr, U. B.** 1978. Regular arrays of macromolecules on bacterial cell walls: structure, chemistry, assembly and function. Int. Rev. Cytol. **53**:103–116.
22. **Sleytr, U. B., and P. Messner.** 1983. Crystalline surface layers on bacteria. Annu. Rev. Microbiol. **37**:311–339.
23. **Sleytr, U. B., and P. Messner.** 1988. Crystalline surface layers in procaryotes. J. Bacteriol. **170**:2891–2897.
24. **Sleytr, U. B., P. Messner, D. Pum, and M. Sára.** 1988. Crystalline bacterial cell surface layers. Springer, Berlin.
25. **Smit, J.** 1986. Protein surface layers of bacteria, p. 343–376. *In* M. Inouye (ed.), Bacterial outer membranes as model systems. John Wiley & Sons, Inc., New York.